J|A|C|S
ARTICLES
Published on Web 12/31/2005

Polyanionic Hydrides from Polar Intermetallics AeE_2 (Ae = Ca, Sr, Ba; E = Al, Ga, In)

Thomas Björling,[‡] Dag Noréus,[‡] and Ulrich Häussermann*[,†,§]

Contribution from the Inorganic Chemistry and Structural Chemistry Departments, Stockholm University, 10691 Stockholm, Sweden

Received July 5, 2005; E-mail: Ulrich.Haussermann@asu.edu

Abstract: The hydrogenation behavior of the polar intermetallic systems AeE_2 (Ae = Ca, Sr, Ba; E = Al, Ga, In) has been investigated systematically and afforded the new hydrides $SrGa_2H_2$ and $BaGa_2H_2$. The structure of these hydrides was characterized by X-ray powder diffraction and neutron diffraction of the corresponding deuterides. Both compounds are isostructural to previously discovered $SrAl_2H_2$ (space group $P\bar{3}m1$, $Z = 1$, $SrGa_2H_2/D_2$: $a = 4.4010(4)/4.3932(8)$ Å, $c = 4.7109(4)/4.699(1)$ Å; $BaGa_2H_2/D_2$: $a = 4.5334(6)/4.5286(5)$ Å, $c = 4.9069(9)/4.8991(9)$ Å). The three hydrides $SrAl_2H_2$, $SrGa_2H_2$, and $BaGa_2H_2$ decompose at around 300 °C at atmospheric pressure. First-principles electronic structure calculations reveal that H is unambiguously part of a two-dimensional polyanion $[E_2H_2]^{2-}$ in which each E atom is tetrahedrally coordinated by three additional E atoms and H. The compounds AeE_2H_2 are classified as polyanionic hydrides. The peculiar feature of polyanionic hydrides is the incorporation of H in a polymeric anion where it acts as a terminating ligand. Polyanionic hydrides provide unprecedented arrangements with both E−E and E−H bonds. The hydrogenation of AeE_2 to AeE_2H_2 takes place at low reaction temperatures (around 200 °C), which suggests that the polyanion of the polar intermetallics ($[E_2]^{2-}$) is employed as precursor.

1. Introduction

Alanates, which are aluminum hydrides of alkali metals (A) or alkaline earth metals (Ae), gained recently a tremendous amount of attention.[1−3] This was triggered by the discovery that some transition metals catalyze the reverse of the two-step decomposition $NaAlH_4 \rightarrow {}^1/_3(Na_3AlH_6) + {}^2/_3Al + H_2 \rightarrow NaH + Al + {}^3/_2H_2$, which suddenly turned long-known $NaAlH_4$ into a state-of-the-art media with 5.6 wt % H-storage capacity. In the past the systems $AAlH_4$ and A_3AlH_6 have been intensively investigated with respect to synthesis, dehydrogenation behavior, structural characterization, and computational modeling of structural stability and physical properties.[4] Further, new alkaline earth metal alanates, such as $BaAlH_5$ and Ae_2AlH_7 (Ae = Sr, Ba), were discovered, and the structure of nanocrystalline $MgAl_2H_8$ was finally solved.[5]

Characteristically, alanates represent fully hydrogenated systems $A_mAe_nAl_oH_{m+2n+3o}$. In 2000, however, Gingl et al. reported the synthesis and structural characterization of peculiar and novel $SrAl_2H_2$.[6] This aluminum hydride compound is not fully hydrogenated and was obtained by hydrogenating the alloy $SrAl_2$ at mild conditions (200 °C, 50 bar H_2 pressure). $SrAl_2$ is usually considered as a member of the large family of Zintl phases that form between active metals (alkali, alkaline earth, or rare earth metals) and a more electronegative p-block metallic or semimetallic element (the E component). According to the Zintl concept, Al is formally reduced by the electropositive Sr and features a three-dimensional four-connected (3D4C) polyanionic network in which each Al atom is surrounded by four neighbors in a distorted tetrahedral fashion. This arrangement fits the electron count of Al^-, which is isoelectronic to Si. In $SrAl_2H_2$ the Al network is maintained, although its dimension is reduced to two. The Al atoms are arranged as puckered graphitic layers where they have three nearest Al neighbors, the vacant coordination is taken by hydrogen. Thus, hydrogen appears to act as a pair of scissors cutting covalent Al−Al bonds and subsequently terminating them (Figure 1). This retains a

[†] Inorganic Chemistry Department.
[‡] Structural Chemistry Department.
[§] Present address: Department of Chemistry and Biochemistry, Arizona State University, Tempe, AZ 85287-1604.

(1) (a) Bogdanovic, B.; Schwickardi, M. J. *J. Alloys Compd.* **1997**, *253*, 1. (b) Bogdanovic, B.; Brand, R. A.; Marjanovic, A.; Schwickardi, M.; Tölle, J. *J. Alloys Compd.* **2000**, *302*, 36. (c) Bogdanovic, B.; Sandrock, G. *MRS Bulletin* **2002**, *September*, 712.
(2) Akiba, E. *Curr. Opin. Solid State Mater. Sci.* **1999**, *4*, 267.
(3) Seayad, A. M.; Antonelli, D. M. *Adv. Mater.* **2004**, *16*, 765.
(4) (a) Hauback, B. C.; Brinks, H. W.; Jensen, C. M.; Murphy, K.; Maeland, A. J. *J. Alloys. Compd.* **2003**, *358*, 142. (b) Hauback, B. C.; Brinks, H. W.; Heyn, R. H.; Blom, R.; Fjellvåg, H. *J. Alloys Compd.* **2005**, *394*, 35. (c) Brinks, W.; Hauback, B. C.; Jensen, C. W.; Zidan, R. *J. Alloys Compd.* **2005**, *392*, 27. (d) Vajeeston, P.; Ravindran, P.; Vidya, R.; Fjellvåg, H.; Kjekshus, A. *Cryst. Growth Design* **2004**, *4*, 471. (e) Lovvik, O. M.; Opalka, S. M.; Brinks, H. W.; Hauback, B. C. *Phys. Rev. B* **2004**, *69*, 134117. (f) Vajeeston P.; P. Ravindran, P.; Fjellvåg, H.; Kjekshus, A. *J. Alloys Compd.* **2003**, *363*, L7. (g) Vajeeston, P.; Ravindran, P.; Vidya, R.; Fjellvåg, H.; Kjekshus, A. *Appl. Phys. Lett.* **2003**, *82*, 2257. (h) Arroyo y de Dompablo, M. E.; Ceder, G. *J. Alloys Compd.* **2004**, *364*, 6.
(5) (a) Zhang, Q.-A.; Nakamura, Y.; Oikawa, K.; Kamiyama, T.; Akiba, E. *Inorg. Chem.* **2002**, *41*, 6547. (b) Zhang, Q.-A.; Nakamura, Y.; Oikawa, K.; Kamiyama, T.; Akiba, E. *Inorg. Chem.* **2003**, *42*, 3152. (c) Zhang, Q.-A.; Nakamura, Y.; Oikawa, K.; Kamiyama, T.; Akiba, E. *Inorg. Chem.* **2002**, *41*, 6941. (d) Zhang, Q. A.; Nakamura, Y.; Oikawa, K.; Kamiyama, T.; Akiba, E. *J. Alloys Compd.* **2003**, *361*, 180. (e) Fichtner, M.; Engel, J.; Fuhr, O.; Glöss, A.; Rubner, O.; Ahlrichs, R. *Inorg. Chem.* **2003**, *42*, 7060;
(6) Gingl, F.; Vogt, T.; Akiba, E. *J. Alloys Compd.* **2000**, *306*, 127.

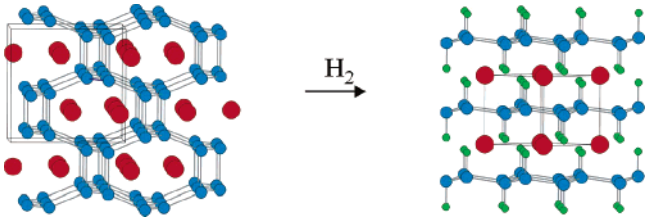

Figure 1. Crystal structures of $SrAl_2$ (left) and $SrAl_2H_2$ (right) viewed along [110]. Red, blue, and green circles denote Sr, Al, and H atoms, respectively.

(two-dimensional) polyanionic structure $[Al_2H_2]^{2-}$ in the hydride with both Al−Al and Al−H bonds and is remarkable against the alanate structures which consist of tetrahedral $[AlH_4]$ or octahedral $[AlH_6]$ entities.

Considering the large number and structural variety of Zintl phases, the immediate question arises: Did the discovery of $SrAl_2H_2$ open up a new class of hydride compounds with unprecedented polyanions consisting of E−E and E−H bonds? Hydrogen displays an electronegativity similar to that of the E component of Zintl phases (i.e. groups 13−15 metallic and semimetallic elements), and thus, the E−H bond should be of covalent nature. This would place the structure and bonding properties of polyanionic hydrides between those of the ionic, salt-like, active metal hydrides and the molecular or polymeric covalent hydrides E_nH_m. Alternatively, polyanionic hydrides can be viewed as intermediates between saline metal hydrides and Zintl phases. The hydrogen content of polyanionic hydrides is comparably low, and thus they may not be appropriate as hydrogen storage materials. However, if physical properties inherent to saline metal hydrides and Zintl phases can be combined in polyanionic hydrides, unexpected prospects are opened by extending hydride materials research beyond the traditional quest for hydrogen storage materials.[7]

We have started to examine systematically the issue of polyanionic hydrides. Specifically, we are interested in exploring which E elements or combinations of E elements form polymeric anions with hydrogen and how hydride formation is influenced by the choice of the countercation. It is important to note that the expression "polyanionic hydride" implies a clear definition applying exclusively to compounds in which hydrogen atoms are part of a polymeric anion. This is in line with the original description of $SrAl_2H_2$ by Gingl et al.[6] and excludes compounds with covalently bonded but separated entities $[EH_n]^{x-}$, such as the alanates and systems such as $KSiH_3$, $AGeH_3$, APH_2 (A = K, Rb, Cs), and A_2PH (A = Rb, Cs), ASH, ASeH.[8] Importantly, this also excludes Zintl phases containing interstitial hydrogen. Such phases were especially described by Corbett et al. and comprise $Ba_5Ga_6H_2$,[9] Ca_3SnH_2 ,[10] and $Ae_5Tt_3H_x$ (Ae = Ca, Sr, Ba; Tt = Si, Ge, Sn)[11] where H is not attached to the semimetal but surrounded exclusively by the cationic component. In this article we report the results of our hydrogenation experiments on AeE_2 (Ae = Ca, Sr, Ba; E = Ga, In), along with thermal behavior and electronic structure characterizations of the obtained compounds. The latter investigations include already known $SrAl_2H_2$. On the basis of this fundamental study we draw general conclusions on bonding and structural and thermal stability of polyanionic hydrides involving metallic group 13 elements as the E component.

2. Experimental Section

Synthesis. All steps of synthesis and sample preparation for diffraction and thermal analysis experiments were performed in an Ar-filled glovebox (O_2 concentration <1 ppm). The binary phases $SrAl_2$, $CaGa_2$, $CaGa_{2+x}$ (x = 0.1−0.2), $SrGa_2$, $BaGa_2$, $SrIn_2$, and $BaIn_2$ were synthesized from the pure elements which where mixed in stoichiometric ratios (total sample amounts between 0.5 and 1.0 g). For preparing $SrAl_2$, elemental mixtures were pressed into pellets, which subsequently were arc melted. This compound melts incongruently, and quantitative yields can only be obtained by the arc-melting procedure. For preparing the gallides and indides, reactant mixtures were transferred into Ta and stainless steel ampules, respectively, which were sealed and placed in a fused quartz Schlenk tube under reduced pressure. The metal mixtures were heated at 200 K/h to 800 °C, held at 800 °C for 24 h, and cooled at 100 K/h to room temperature. The binary intermetallics were obtained as ingots that were ground, and the powdered samples were used for subsequent characterization and hydrogenation. For their hydrogenation the intermetallic compounds were loaded in corundum crucibles, which were placed in stainless steel autoclaves. Reactions were carried out at hydrogen pressures around 50 bar and at temperatures varying between 150 and 400 °C. All products obtained (intermetallics and hydrides) were characterized by Guinier powder diagrams (Cu Kα; Si standard) and their Ae:E ratios were confirmed with the EDX (energy-disperse X-ray) method in a JEOL 820 scanning electron microscope.

Structural Characterization. Lattice parameters of the prepared intermetallics and their hydrides were obtained from least-squares refinement of measured and indexed lines of the corresponding Guinier powder diffractograms.[12] The considered phases AeE_2 and $CaGa_{2+x}$ (x = 0.1−0.2) are all described in the literature.[13] In some cases we undertook a structural reinvestigation from single-crystal X-ray diffraction data. Atomic positions of $SrGa_2H_2$ and $BaGa_2H_2$ were determined from Rietveld profile refinements of neutron powder diffraction data[14] from deuterized samples measured at Studsvik Neutron Research Laboratory, Sweden (room temperature, λ = 1.4700 Å for $SrGa_2D_2$ and 1.5514 Å for $BaGa_2D_2$, data resolution $\Delta d/d = 2 \times 10^{-3}$). These samples were obtained by reacting $SrGa_2$ and $BaGa_2$ with deuterium at a pressure of 50 bar and at a temperature of 200 °C for 4 days. The $SrGa_2D_2$ sample contained some $SrGa_2$, which was due to insufficient supply of D_2 during the reaction. The $BaGa_2D_2$ sample contained a small amount of $BaGa_4$, which occurred as a byproduct during the synthesis of $BaGa_2$. Due to overlapping reflections, a multiphase refinement was performed. Initial values for the atomic coordinates were taken from $SrAl_2H_2$. The results are presented in Tables 1 and 3.

Thermal Investigations. The thermal behavior of powdered samples of $SrAl_2H_2$, $SrGa_2H_2$, and $BaGa_2H_2$ was investigated by differential thermal analysis (DTA-TG, Setaram Labsys 1600). Samples were placed in a steel container, which were sealed with gold foil to prevent

(7) Björling, T.; Noréus, D.; Jansson, K.; Andersson, M.; Leonova, E.; Edén, M.; Hålenius, U.; Häussermann, U. *Angew. Chem., Int. Ed.* **2005**, *44*, 7269.
(8) (a) Mundt, O.; Becker, G.; Hartmann, H. M.; Schwarz, W. *Z. Anorg. Allg. Chem.* **1989**, *572*, 75. (b) Thirase, G.; Weiss, E.; Hennig, H. J.; Lechert, H. *Z. Anorg. Allg. Chem.* **1975**, *417*, 221. (c) Bergerhoff, G.; Schultze-Rhonhof, E. *Acta Crystallogr.* **1962**, *15*, 420. (d) Jacobs, H.; Hassiepen, K. M. *Z. Anorg. Allg. Chem.* **1985**, *531*, 108. (e) Somer, M.; Carrillo-Cabrera, W.; Peters, E.-M.; Peters, K.; von Schnering, H. G. *Z. Kristallogr.—New Crystal Struct.* **1997**, *212*, 299. (f) von Schnering, H. G.; Somer, M.; Peters, K.; Carrillo-Cabrera, W.; Grin, Y. *Z. Kristallogr.—New Crystal Struct.* **2001**, *216*, 42.
(9) Henning, R. W.; Alejandro Leon-Escamilla, E.; Zhao, J.-T.; Corbett, J. D. *Inorg. Chem.* **1997**, *36*, 1282.
(10) Huang, B.; Corbett J. D. *Inorg. Chem.* **1997**, *36*, 3730.
(11) Alejandro Leon-Escamilla, E.; Corbett, J. D. *J. Solid State Chem.* **2001**, *159*, 149.
(12) Werner, P.-E. *Ark. Kemi* **1969**, *31*, 513.
(13) Villars, P.; Calvert, L. D. *Pearsons Handbook of Crystallographic Data for Intermetallic Compounds*, 2nd ed.; ASM International: Materials Park, OH, 1991; Desk Edition, 1997.
(14) Rodriguez-Carvajal, J. FULLPROF: A Program for Rietveld Refinement and Pattern Matching Analysis. *Abstracts of the Satellite Meeting on Powder Diffraction of the XV Congress of the IUCr*; Toulouse, France, 1990; p 127.

Table 1. Refinement Results[a] for $AeGa_2H_2/D_2$

compound	$SrGa_2H_2/D_2$	$BaGa_2H_2/D_2$
space group, *Z*	$P\bar{3}m1$, 1	$P\bar{3}m1$, 1
a, Å	4.4010(4)/4.3932(8)	4.5334(6)/4.5286(5)
c, Å	4.7109(4)/4.699(1)	4.9069(9)/4.8991(9)
V, Å^3	79.02/78.54	87.33/87.01
T, K	295	295
R_{Bragg}	4.73	4.51
R_p	11.9	10.4
R_{wp}	12.0	11.5
Ae 1a/B_{eq}	0, 0, 0/0.45(10)	0, 0, 0/0.61(7)
E 2d/B_{eq}	1/3, 2/3, 0.4656(7)/0.17(6)	1/3, 2/3, 0.4680(4)/0.78(4)
D 2d/B_{eq}	1/3, 2/3, 0.1067(8)/2.03(8)	1/3, 2/3, 0.1232(4)/1.75(5)

[a]Cell parameters obtained from X-ray data.

Table 2. Computationally Relaxed Structural Parameters for AeE_2H_2

	$SrAl_2H_2$[a]	$SrGa_2H_2$	$BaGa_2H_2$
a, Å	4.5289 (4.5283)	4.4104	4.5604
c, Å	4.7248 (4.7215)	4.7291	4.9700
E (1/3, 2/3, z)	0.4614 (0.4589)	0.4658	0.4703
H (1/3, 2/3, z)	0.0988 (0.0976)	0.1061	0.1287

[a]Experimental values for $SrAl_2H_2$ according to ref 6 are given in parentheses.

Table 3. Selected Interatomic Distances (Å) and Angles (deg) in AeE_2D_2

		$SrAl_2D_2$[a]	$SrGa_2D_2$	$BaGa_2D_2$
Ae−D	6x	2.653(1)	2.586(1)	2.683(1)
Ae−E	6x	3.394(2)	3.350(2)	3.477(1)
Ae−E	6x	3.654(2)	3.569(2)	3.692(2)
E−D	1x	1.706(4)	1.687(5)	1.689(3)
E−E	3x	2.641(1)	2.557(1)	2.6334)
D−E	1x	1.706(4)	1.687(5)	1.689(3)
D−Ae	3x	2.653(1)	2.586(1)	2.683(1)
D−D	3x	2.770(1)	2.727(3)	2.880(2)
E−E−E		117.88(2)	118.42(6)	118.60(4)
E−E−D		98.5(2)	97.3(1)	96.8(1)

[a] Values for $SrAl_2D_2$ are taken from ref 6.

exposure to air and moisture, and the temperature was raised from 40 to 400 °C. The experiments were performed under a flow of dry Ar and with a temperature increase rate of 5 K/min. It should be pointed out that these investigations do not monitor hydride decomposition strictly at thermodynamic equilibrium conditions.

Electronic Structure Calculations. Total energy calculations for AeE_2 and AeE_2H_2 (Ae = Ca, Sr, Ba; E = Al, Ga, In) were performed in the framework of the frozen core all-electron Projected Augmented Wave (PAW) method,[15] as implemented in the program VASP.[16] The energy cutoff was set to 500 eV. Exchange and correlation effects were treated by the generalized gradient approximation (GGA), usually referred to as PW91.[17] The integration over the Brillouin zone was done on special k points determined according to the Monkhorst−Pack scheme.[18] Total energies were converged to at least 1 meV/atom. Structural parameters were relaxed until forces had converged to less than 0.01 eV/Å. The computationally obtained parameters for $SrAl_2H_2$, $SrGa_2H_2$, and $BaGa_2H_2$ are listed in Table 2.

3. Results

Zintl Phases AeE_2. The discovery of the prototype polyanionic hydride $SrAl_2H_2$ from $SrAl_2$ prompted the investigation of the hydrogenation behavior of the related phases AeE_2 (Ae = Ca, Sr, Ba; E = Ga, In). These six isoelectronic compounds occur in three different structures (Figure 2). $SrGa_2$ and $BaGa_2$ crystallize with the hexagonal AlB_2-type ($P6_3/mmm$), $CaGa_2$, $CaIn_2$, and $SrIn_2$ with the hexagonal $CaIn_2$-type ($P6_3/mmc$), and $BaIn_2$ with the orthorhombic $CeCu_2$-type (*Imma*).[19,20] Additionally, there exists slightly nonstoichiometric $CaGa_{2+x}$ with the AlB_2 structure.[21] The three structure types are closely related.[19] In the simple AlB_2 structure E atom hexagon layers are stacked on top of each other, and Ae atoms are sandwiched between two hexagon rings of neighboring layers. The $CaIn_2$ and $CeCu_2$ structures have 3D4C E atom networks and are easily derived from the AlB_2-type. In the $CaIn_2$-type E atom hexagon layers are corrugated as in gray As and connected as in hexagonal diamonds. In the $CeCu_2$-type E atom hexagon layers are corrugated as in black P (which yields a smoother corrugation compared to $CaIn_2$) and connected to give a ladder of four-membered rings.

In systems AeE_2 the group 13 E atoms are formally singly charged and thus isoelectronic to a group 14 element. The formation of 3D4C polyanionic networks for compounds with (distorted) tetrahedrally coordinated E atoms is reasonable. This holds also for AlB_2-type $SrGa_2$ and $BaGa_2$ when considering the hexagon layers electronically as graphitic layers. Thus, these compounds are apparently charge-balanced and conform to the Zintl concept although they adopt different structures. $AeAl_2$ displays a somewhat different structural chemistry. Only $SrAl_2$ crystallizes with a structure that agrees with the Zintl concept ($CeCu_2$-type).[22] $CaAl_2$ forms the cubic Laves phase structure $MgCu_2$ and $BaAl_2$ does not exist but decomposes into complex $Ba_{21}Al_{40}$ and $BaAl_4$.[23]

Hydrogenation reactions. The prepared phases $CaGa_2$, $CaGa_{2+x}$, $SrGa_2$, $BaGa_2$, $CaIn_2$, $SrIn_2$, and $BaIn_2$ were exposed to a hydrogen atmoshphere of 50 bar at various temperatures. Additionally we included $SrAl_2$ in our investigation. The result of these reaction series is compiled in Scheme 1. For $SrAl_2$, $SrGa_2$, and $BaGa_2$ we observe hydride formation at temperatures between 170 and 200 °C. These hydrides corresponds to AeE_2H_2. At hydrogenation temperatures between 250 and 300 °C $AeGa_2H_2$ decomposes upon formation of AeH_2 and $AeGa_4$. This is in contrast to $SrAl_2H_2$, which is further hydrogenated to Sr_2AlH_7.[5a,5b] Sr_2AlH_7 represents a fully hydrogenated alanate system and apparently there is no equivalent for gallium compounds. $CaIn_2$-type $CaGa_2$ and AlB_2-type $CaGa_{2+x}$ do not yield any hydride but decompose immediately into roentgen-amorphous CaH_2 and monoclinic $CaGa_4$. $CaIn_2$, and $SrIn_2$ remain unaffected upon hydrogenation up to temperatures of 400 °C. Most likely $CaIn_2$ and $SrIn_2$ decompose into AeH_2 and E at higher temperatures. This decomposition is already observed for $BaIn_2$ at very low temperatures (around 200 °C). The low melting temperature of elemental Ga prompted us to attempt

(15) (a) Blöchl, P. E. *Phys. Rev. B* **1994**, *50*, 17953. (b) Kresse, G.; Joubert, J. *Phys. Rev. B* **1999**, *59*, 1758.
(16) (a) Kresse, G.; Hafner, J. *Phys. Rev. B* **1993**, *47*, 558. (b) Kresse, G.; Furthmüller, J. *Phys. Rev. B* **1996**, *54*, 11169.
(17) Perdew, J. P.; Wang, Y. *Phys. Rev. B* **1992**, *45*, 13244.
(18) Monkhorst; H. J.; Pack, J. D. *Phys. Rev. B* **1972**, *13*, 5188.
(19) Nuspl, G.; Polborn, K.; Evers, J.; Landrum, G. A.; Hoffmann, R. *Inorg. Chem.* **1996**, *35*, 6922.
(20) (a) Bruzzone, G.; Bonino, G. B. *Atti Accad. Nat. Lincei* **1970**, *48*, 235. (b) Iandelli, A. *Z. Anorg. Allg. Chem.* **1964**, *330*, 221. (c) Bruzzone, G. *Bollettino Scientifico della Facolta di Chimica Industriale di Bologna* **1966**, *24*, 113. (d) Iandelli, A. *J. Less-Common Met.* **1987**, *135*, 195.
(21) Bruzzone, G.; Fornasini, M. L.; Merlo, F. *J. Less-Common Met.* **1989**, *154*, 67.
(22) (a) Nagorsen, G.; Posch, H.; Schäfer, H.; Weiss, A. *Z. Naturforsch.* **1969**, *24b*, 1191. (b) Cordier, G.; Czech, E.; Schäfer, H. *Z. Naturforsch.* **1982**, *37b*, 1442.
(23) Amerioun, S.; Yokosawa, T.; Lidin, S.; Häussermann, U. *Inorg. Chem.* **2004**, *43*, 4751.

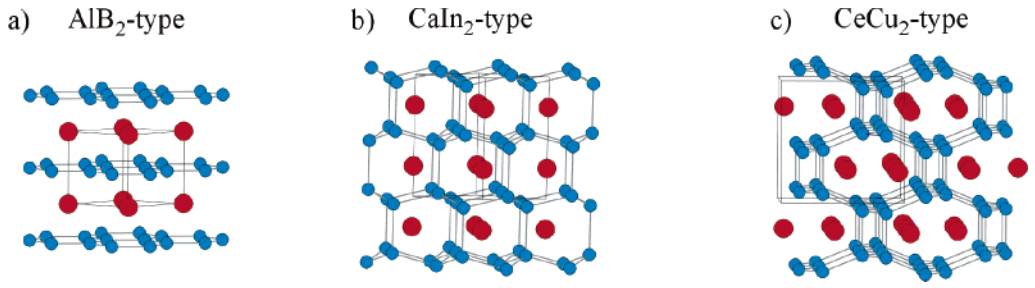

Figure 2. Crystal structures of AlB_2-type $SrGa_2$, $BaGa_2$ (a) $CaIn_2$-type $CaGa_2$, $CaIn_2$, $SrIn_2$ (b) and $CeCu_2$-type $SrAl_2$, $BaIn_2$ (c). Red and blue circles denote Ae and E atoms, respectively.

Scheme 1

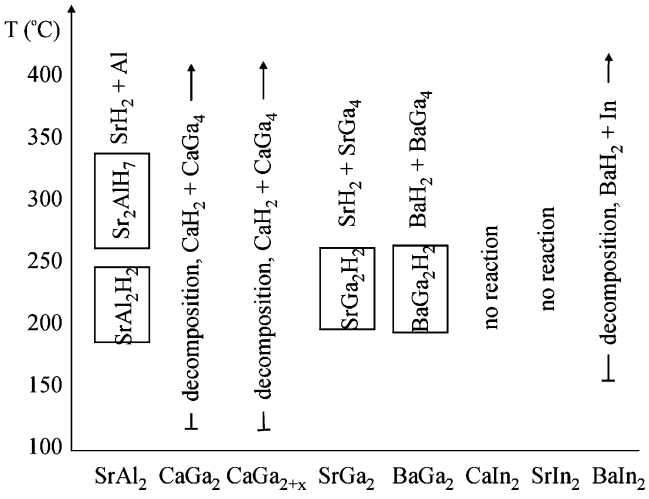

the synthesis of $AeGa_2H_2$ from stoichiometric mixtures of AeH_2 and Ga under a hydrogen pressure of 50 bar. However, already at reactions temperatures as low as 100 °C $BaAl_4$-type $AeGa_4$ was obtained, which behaves completely inert to hydrogen.[24] In general, the polyanionic hydrides AeE_2H_2 are highly moisture sensitive and decompose rapidly when exposed to air. For the sake of completeness we note that the Laves phase $CaAl_2$ has been the subject of earlier hydrogenation experiments.[25] This compound decomposes into CaH_2 and Al at high temperatures. $Ba_{21}Al_{40}$ (previously denoted as Ba_7Al_{13}) has a structure closely related to the Laves phases[23] and affords the alanates $BaAlH_5$ and Ba_2AlH_7 when exposed to a hydrogen atmosphere under elevated temperature.[5c,5d]

Hydride structures. The structures of $SrGa_2H_2$ and $BaGa_2H_2$ were established from the Rietveld refinement of neutron diffraction powder data. Both compounds are isostructural to already reported $SrAl_2H_2$ (cf. Figure 1).[6] In the trigonal structure type of $SrAl_2H_2$ (space group $P\bar{3}m1$) E atoms form slightly puckered graphitic layers. Additionally each E atom is coordinated to one hydrogen atom. This yields a two-dimensional polyanion $[E_2H_2]^{2-}$ which is formally electron precise. The occurrence of polyanions with both, E−E and E−H bonds has not been observed earlier and is the unique feature of polyanionic hydrides. Al−H and Ga−H distances are very similar, around 1.70 Å, Al−Al and Ga−Ga distances are in a range typically observed for Zintl phases containing polyanions with E−E single bonds (Table 3).

(24) We also performed a hydrogenation study of $BaAl_4$-type polar intermetallics AeE_4 (Ae = Sr, Ba, E = Al, Ga). These compounds do not react with hydrogen under the autoclave conditions employed (maximum hydrogen pressure 70 bar, maximum temperature 700 °C).

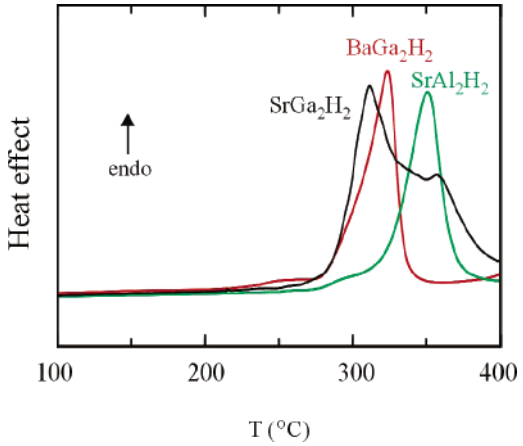

Figure 3. DTA heating curves for $SrAl_2H_2$, $SrGa_2H_2$, and $BaGa_2H_2$.

It is interesting to mention that the formation of $SrGa_2H_2$ was difficult to recognize from the X-ray powder pattern because $SrGa_2$ and $SrGa_2H_2$ have hexagonal cells with very similar axes (a = 4.36 and 4.40 Å, c = 4.70 and 4.71 Å, respectively). However, there are small but significant intensity differences for a few reflections (e.g. 102, 212, and 104), which are a consequence of the different arrangement of Ga atoms in the two structures (planar hexagon layers vs puckered ones). The formation of $SrAl_2H_2$ from $SrAl_2$ is accompanied by a volume increase of 8.9 $Å^3$/Z, whereas the volume changes connected with the hydrogenation of $SrGa_2$ and $BaGa_2$ are very small (increase by about 1 $Å^3$/Z). This different behavior can be explained by fact that the hexagon nets formed by Ga atoms in AlB_2-type $AeGa_2$ are widely separated, whereas in $CeCu_2$-type $SrAl_2$ the corresponding layers of Al are connected by bonds and thus much closer together (cf. Figure 2). Upon hydride formation these bonds are broken, and the layers move farther apart when terminated by hydrogen.

Thermal Stability. Figure 3 displays DTA heating curves for AeE_2H_2 at atmospheric pressure (inert gas). We observe a sharp endothermic rise around 280 °C for the gallium compounds. For $SrAl_2H_2$ a small thermal effect occurs in this temperature range, which may indicate the onset of hydrogen desorption. The main desorption, however, should coincide with the steep rise at about 320 °C. The three hydrides display a very similar thermal stability; their decomposition takes place at around 300 °C. For $SrGa_2H_2$ a second endothermic effect is seen at around 350 °C, for $BaGa_2H_2$ at around 450 °C (not included in Figure 3). We attribute this effect to further reactions leading to the formation of $BaAl_4$-type $AeGa_4$. As a matter of

(25) (a) Veleckis, E. *J. Less-Common Met.* **1981**, *80*, 241. (b) Zhang, Q. A.; Enoki, H.; Akiba, E. *J. Alloys Compd.* **2001**, *322*, 257.

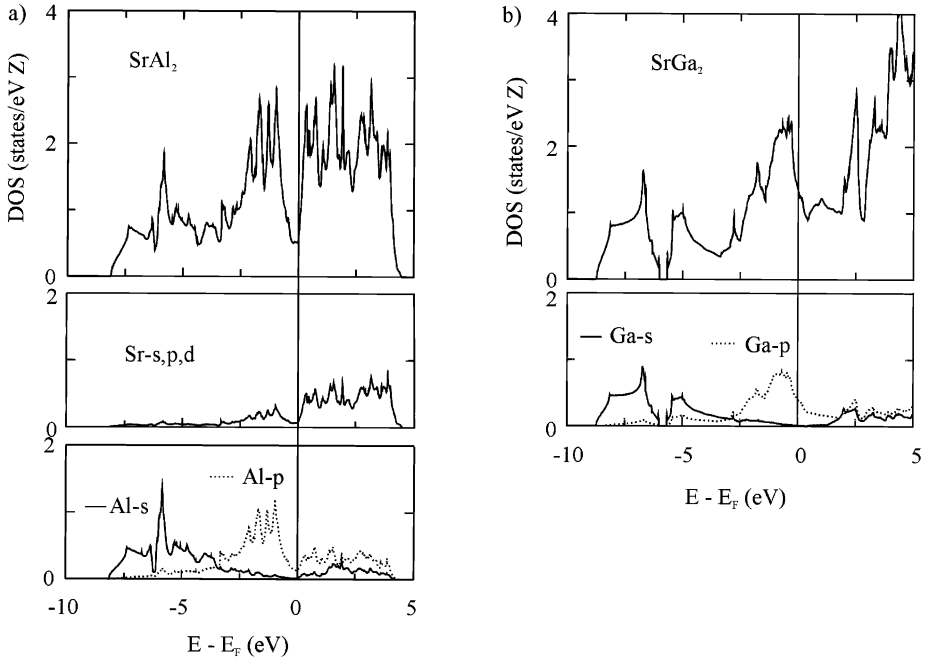

Figure 4. Electronic density of states (DOS) for $CeCu_2$-type $SrAl_2$ (a) and AlB_2-type $SrGa_2$ (b).

fact, from powder X-ray analysis we identify a considerable amount of AeE_4 in all three systems after atmospheric pressure decomposition.

4. Discussion

The discovery of $SrGa_2H_2$ and $BaGa_2H_2$ shows that $SrAl_2H_2$ is not a singularity and that polyanionic hydrides may indeed represent a wider class of compounds. Importantly, polyanionic hydrides AeE_2H_2 were obtained from the hydrogenation of phases AeE_2 only when applying low reaction temperatures (180−230 °C). Higher temperatures eventually result in a mixture of AeH_2 and $BaAl_4$-type AeE_4 or AeH_2 and E metal. (In the case of $SrAl_2H_2$ an intermediate alanate is obtained). The synthesis reaction $AeH_2 + 2Ga$, which in principle allows low reaction temperatures because of the low melting point of Ga, does not afford polyanionic hydrides at the conditions applied by us. Also, it is not possible to obtain polyanionic hydrides from the compounds $CaAl_2$ and $Ba_{21}Al_{40}$ with Laves phase structures. These observations point strongly to the fact that the polyanion $[E_2]^{2-}$, which is present in Zintl phases AeE_2, is utilized as precursor in the hydrogenation reaction. In this case the E−E bonded part of final $[E_2H_2]^{2-}$ is completely preformed, and the hydrogenation reaction—leading to covalent E−H bond formation—can take place at mild, low-temperature conditions. The prerequisite for a precursor reaction is the possibility to preserve the countercation arrangement of the Zintl phase in the hydride. As a matter of fact, the $SrAl_2H_2$ structure is closely related to that of the parent Zintl phases. The insertion of hydrogen into AeE_2 induces only a minor rearrangement of the metal atoms and is similar to a topotactic reaction.

For the formation of $AeGa_2H_2$ from AlB_2-type $AeGa_2$ hydrogen is added to a three-bonded, sp^2-hybridized E^- entity, which changes into an sp^3-hybridized one upon binding to H. The arrangement of Ae atoms is not affected at all, and the space group of the hydride ($P\bar{3}m1$) is a translationengleiche (*t*2) subgroup of the precursor (*P*6/*mmm*). The Ga−Ga distances in $AeGa_2$ are 2.52 and 2.57 Å for Ae = Sr and Ba, respectively.[26] In $AeGa_2H_2$ they are widened to 2.56 and 2.63 Å for Ae = Sr and Ba, respectively. This is in accord with the idea that the stronger bonded Ga−Ga bonded π-system is destroyed in the precursor polyanion upon hydrogenation and the Ga atoms become four-coordinated in the hydride. In the case of the pair $SrAl_2/SrAl_2H_2$, puckered Al hexagon layers are present in both structures (cf. Figure 1). In $CeCu_2$-type $SrAl_2$ these layers are connected. Al−Al distances are 2.776 and 2.783 Å within the layers and are somewhat longer, 2.882 Å, between layers.[27] Upon hydride formation the long, layer-connecting bonds become dissected and subsequently terminated by hydrogen. The Al atoms in the corrugated hexagon layer and the Sr atoms rearrange slightly. Although the metal atom arrangements in the $CeCu_2$-type precursor and the trigonal hydride are very similar, their space group symmetries (*Imma* and $P\bar{3}m1$, respectively) can only be related via hexagonal *P*6/*mmm* (AlB_2).[28] The Al−Al distance in $SrAl_2H_2$ is considerably reduced (2.64 Å) compared to the interlayer distances in $SrAl_2$ and corresponds much closer to what is considered an Al−Al single-bonded distance (cf. Table 3).

In the next step we compare the electronic structures of formally electron-precise AeE_2 and AeE_2H_2.[29] For this we computed the electronic density of states (DOS) at the theoreti-

(26) The cell parameters for AlB_2-type $AeGa_2$ obtained by us are $a = 4.3614(7)$ Å, $c = 4.696(1)$ Å for Ae = Sr and $a = 4.4323(3)$ Å, $c = 5.0823(8)$ Å for Ae = Ba. The Ga−Ga distance is $(\sqrt{3}a)/3$.

(27) These distances are based on our reinvestigation of the crystal structure of $SrAl_2$ from single-crystal X-ray data: space group *Imma*; $a = 4.7954(6)$ Å, $b = 7.8956(9)$ Å, $c = 7.953(1)$ Å; Sr 4e (0, 1/4, 0.05047(4): Al 8h (0, 0.9325(1), 0.3388(1)). The parameters differ slightly from the data presented in the original reports (ref 20). The reinvestigation of the crystal structure of $SrAl_2$ also confirmed the stoichiometric composition of this compound although it was prepared by high-temperature arc-melting.

(28) Hoffmann, R.-D.; Pöttgen, R. *Z. Kristallogr.* **2001**, *216*, 127.

(29) A comparison of the electronic structures of $SrAl_2$ and $SrAl_2H_2$ has been recently performed by Orgaz and Aburto (Orgaz, E.; Aburto, A. *Int. J. Quantum Chem.* **2005**, *101*, 783) on the basis of LAPW calculations and the experimental crystal structures. While the DOS for $SrAl_2H_2$ resembles strongly our result, the one for $CeCu_2$-type $SrAl_2$ looks completely different and does not correspond to what is expected for a polar intermetallic compound.

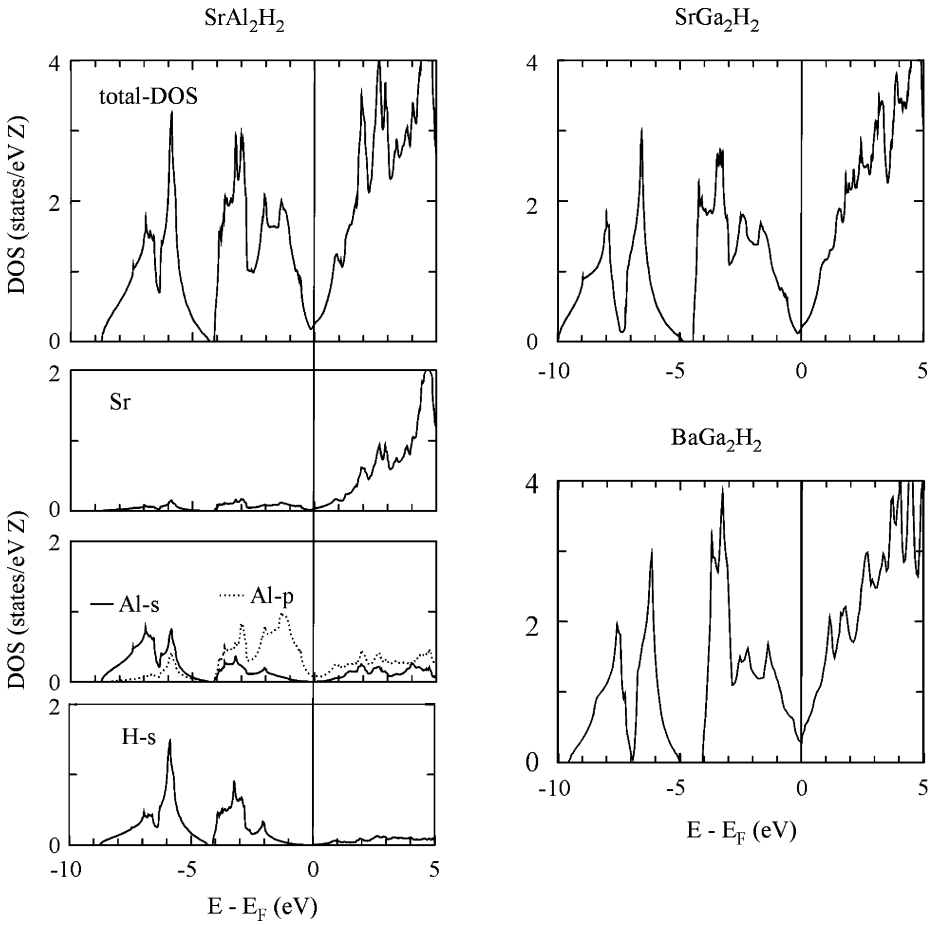

Figure 5. DOS for $SrAl_2H_2$, $SrGa_2H_2$, and $BaGa_2H_2$. The distribution of the Ae, E, and H site-projected DOS is very similar for the three compounds and only shown for $SrAl_2H_2$.

cally obtained equilibrium structures. The results are shown in Figures 4 and 5. The DOS of $SrAl_2$ (Figure 4a) displays a pseudogap, which separates occupied from nonoccupied states. Al states dominate the DOS below the Fermi level, and the pseudogap is a consequence of strong covalent Al−Al interactions within the polyanionic network. To the contrary, in the DOS for the AlB_2-type gallides this pseudogap is absent, and the value of the density of states at the Fermi level is rather high (Figure 4b). The metallic behavior of $CeCu_2$-type $SrAl_2$ and AlB_2-type $AeGa_2$ is due to a large portion of E−p bands crossing the Fermi level. This is especially the case for the latter compounds. As a matter of fact, the electronic structure of a graphitic layer is not recognized in the occupied bands, as perhaps anticipated for charge-balanced AlB_2-type $AeGa_2$. This is simply because pπ- and pσ-type bands are not energetically separated. Thus, although formally charge-balanced, the electronic structure of intermetallic systems AeE_2 does not completely conform to what is expected for Zintl phases, and therefore, they should be classified more appropriately as polar intermetallics. The presence of substantial polarity is recognized in the low contribution of Sr atoms to the occupied states, which sharply rises above the Fermi level.

The electronic structures of $SrAl_2H_2$ and $AeGa_2H_2$ are virtually identical, but rather different from those of the underlying intermetallics. First we observe a very pronounced pseudogap at the Fermi level. Compared to the precursor materials the hydrides are poorer metals. Thus, the incorporation of hydrogen in the polyanionic E atom network enhances its polyanionic character. Second, in the hydrides the E atom s band is detached from the p band. The contribution of H is mainly into the intermediate energy regions of the DOS (between −6.5 and −2 eV), which are the parts where E atom s and p bands strongly mix. The hybridization of H s and E s,p states strongly indicates that H is covalently bonded to the Al framework and thus part of the 2D polyanion $[E_2H_2]^{2-}$. This is corroborated by the analysis of the charge density ρ. In Figure 6 ρ and the difference density $\Delta\rho$ are compared for the pair $SrGa_2$ and $SrGa_2H_2$ in the (110) plane. The charge density distribution shows bond critical points associated with high values of ρ along the Ga−Ga distance in both systems, and additionally along the Ga−H distance in the hydride. This is characteristic for covalent bonding. The polar character of both compounds is revealed in the $\Delta\rho$ map, which clearly shows charge depletion around Sr and accumulation between the polyanion-forming atoms. Concerning the Ga−H bond $\Delta\rho$ suggests substantial charge accumulation around the position of the proton. Undoubtedly, H possesses a higher electronegativity than Ga, and the Ga−H bond is polarized. However, this situation appears exaggerated in the $\Delta\rho$ map because of the absence of core electrons in H.

Finally, modern first-principles methods allow in principle the quantification of structural stability and even reaction energies. We computed energies of formation (i.e., formation enthalpies at zero temperature) for all combinations AeE_2H_2 and considered the two formation reactions $AeE_2 + H_2 \rightarrow AeE_2H_2$ (1) and $AeH_2 + 2E \rightarrow AeE_2H_2$ (2). We point out that the applied

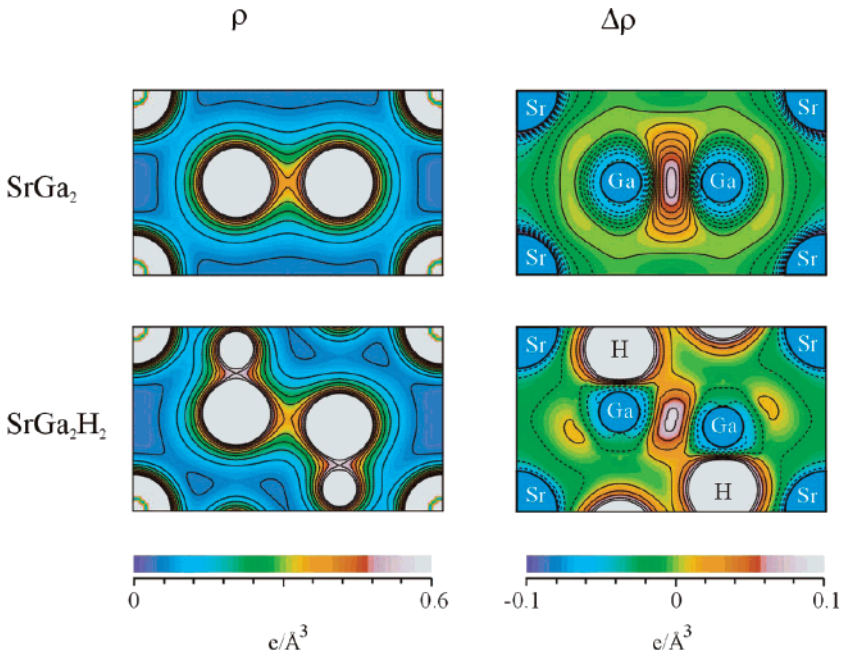

Figure 6. Charge density ρ and difference density $\Delta\rho$ (crystalline - superposed atomic density) distribution in the (110) plane for $SrGa_2$ and $SrGa_2H_2$.

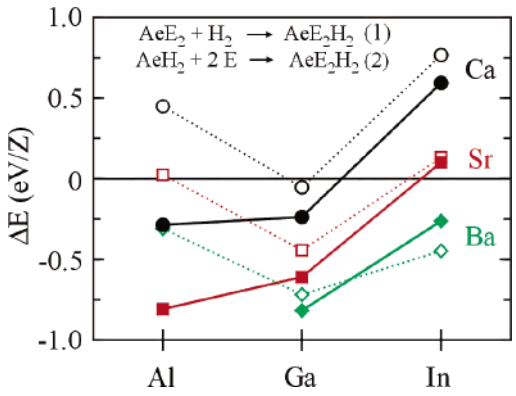

Figure 7. Computed zero-temperature formation energies for systems AeE_2H_2 (Ae = Ca, Sr, Ba; E = Al, Ga, In). The reactions $AeE_2 + H_2$ (1, solid symbols) and $AeH_2 + 2E$ (2, open symbols) were considered. A precursor $BaAl_2$ does not exist; thus, the reaction $BaAl_2 + H_2$ was not taken into account.

computational method very well reproduces the experimental structural parameters of AeE_2H_2. This is shown in Table 2. The obtained energies of formation are compiled in Figure 7. Four important results can be extracted from this figure: (i) At least one of the zero-temperature formation energies, (1) or (2), is negative for all systems, except for $CaIn_2H_2$ and $SrIn_2H_2$. Reaction 2 yields typically a more positive value (except for $BaIn_2H_2$). (ii) $SrAl_2H_2$ is hardly stable against disproportionation into $SrH_2 + 2Al$ (reverse formation reaction 2). Hypothetical $CaAl_2H_2$ would be stable against decomposition into $CaAl_2 + H_2$, but not against $CaH_2 + 2Al$. (iii) Ba compounds, where the 2D $[E_2H_2]^{2-}$ layers are separated most, are more stable with respect to disproportionation into $(AeE_2 + H_2)$ or $(AeH_2 + 2E)$ than are SrE_2H_2 and CaE_2H_2 systems. Also, In compounds display a lower stability with respect to these disproportionations than Al and Ga compounds. (iv) The experimentally obtained compounds $SrAl_2H_2$, $SrGa_2H_2$, and $BaGa_2H_2$ have the lowest zero-temperature formation energies (1), around -0.75 eV/Z.

The zero-temperature formation energy (1) represents only a crude estimate of stability for AeE_2H_2 because the hydrogenation reaction involves a gaseous species. This leads to a decisive entropy contribution when, more appropriately, the Gibbs free energy is considered.[30] In a recent paper Ke and Tanake investigated the decomposition reaction for $NaAlH_4$ and Na_3AlH_6 and found that the entropy contribution $T\Delta S$ to the reaction is approximately equal to the entropy contribution of the H_2 gas molecule produced in that reaction.[31] This is an important result since this contribution can be calculated from thermochemical data. The temperature-dependent Gibbs free energy for a H_2 gas molecule at 1 atm with respect to 0 K is -0.32 eV at 300 K and -0.76 eV at 600 K.[31] Assuming that sodium alanates and AeE_2H_2 systems behave similarly, the first value would imply that only $SrAl_2H_2$, $SrGa_2H_2$, and $BaGa_2H_2$ are stable with respect to $AeE_2 + H_2$ at atmospheric pressure around room temperature. The second value would indicate a decomposition of these three hydrides at temperatures around 600 K, which is in good agreement with the results of our thermal analysis experiments.

5. Conclusions

The recent discovery of the peculiar, polyanionic hydride $SrAl_2H_2$ by Gingl et al.[6] stimulated the search for further examples of such hydrides to prove their wider significance. A general study of the hydrogenation behavior of polar intermetallic compounds AeE_2 (Ae = Ca, Sr, Ba; E = Ga, In) afforded $SrGa_2H_2$ and $BaGa_2H_2$, which are isostructural to $SrAl_2H_2$. A further example of a polyanionic hydride is SrAlSiH.[7] The close structural relationship between AeE_2 and AeE_2H_2 together with the low reaction temperatures employed during hydrogenation suggest that the polyanion $[E_2]^{2-}$ present in the starting material acts as a precursor. Then there are two mechanisms for AeE_2H_2 formation: Either E−E contacts in a 3D4C framework of the precursor material are partly dissected and subsequently terminated by H, or H is added to a formally sp^2

(30) Additionally for hydrides the zero-point energy can give a substantial contribution to formation energies.
(31) Ke, X.; Tanaka, I. *Phys. Rev. B* **2005**, *71*, 024117.

Scheme 2

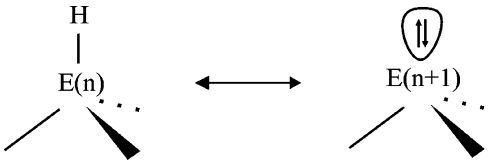

hybridized E atom entity which changes into an sp^3 hybridized one upon binding to H.

The peculiar feature of polyanionic hydrides is the incorporation of H as terminating ligand in a polymeric anion composed of p-block metal or semimetal atoms E (e. g., Al, Ga, In, Si, Ge, Sn, P, As, Sb). This provides unprecedented arrangements with both E−E and E−H bonds. Entities E(n)−H are isoelectronic to entities E(n+1): (see Scheme 2). Therefore the metal/semimetal arrangement in polyanionic hydrides $M_xE(n)_yH_z$ may often correspond to crystal structures of Zintl phases $M_xE(n)_{y-z}E(n+1)_z$ (M = countercation, E(n) = element n). Indeed, the metal arrangement in $AeE(13)_2H_2$ corresponds to the $CeCd_2$ structure type which is adopted by several alkaline earth metal silicides and germanides. This important relationship was already pointed out by Gingl et al.[6] Polyanionic hydrides may be considered as a novel class of hydrides. However, their compositional potential is virtually unexplored. For instance, at the moment it is not clear whether polyanionic hydrides with entities E(n > 13)−H exist and how hydride formation depends on the choice and especially the concentration of the countercation. The hydrogenation of $AeE(13)_2$ yields only a small number of Zintl-phase hydrides. Most likely, their formation requires that the polyanion is preformed in $Ae(E13)_2$. Still, this need not to be a general condition for the formation of polyanionic hydrides. The stability of hydrides $AeE(13)_2H_2$ with respect to the precursor materials and H_2 can be assessed correctly from first-principles total energy calculations, and we believe that such calculations will be a helpful tool for the further exploration of polyanionic hydrides.

Acknowledgment. This work has been supported by the Swedish Research Council (VR). Additionally the European Union is acknowledged for financial support through the European Project HYSTORY with the contract number ENK6-CT-2002-00600.

Supporting Information Available: Rietveld fits to the neutron powder diffraction pattern of $SrGa_2D_2$ and $BaGa_2D_2$. This material is available free of charge via the Internet at http://pubs.acs.org.

JA054456Y